

Feedback Control of Heterogeneous Janus Particles and 3D Motion

Louis William Rogowski, Xiao Zhang, Li Huang, Anuruddha Bhattacharjee, Jung Soo Lee, Aaron Becker, Min Jun Kim

Abstract— This paper presents 2D feedback control and open loop 3D trajectories of heterogeneous chemically catalyzing Janus particles. Self-actuated particles have enormous implications for both *in vivo* and *in vitro* environments, which make them a diverse resource for a variety of medical and assembly applications. Janus particles, consisting of cobalt and platinum hemispheres, can self-propel in hydrogen peroxide solutions due to platinum’s catalyzation properties. These particles are directionally controlled using static magnetic fields produced from a triaxial Helmholtz coil system. Since the magnetization direction of the Janus particles is often heterogeneous, and thereby not consistent with the propulsion direction, this creates a unique opportunity to explore the motion effects of these particles under feedback control and open loop 3D control. Using a modified closed loop controller, Janus particles with magnetization both closely aligned and greatly misaligned to the propulsion vectors, were instructed to perform complex trajectories. These trajectories were then compared between trials to measure both consistency and accuracy. The effects of increasing offset between the magnetization and propulsion vectors were also analyzed. The effects this heterogeneity had on 3D motion is also briefly discussed. It is our hope going forward to develop a 3D closed loop control system that can retroactively account for variations in the magnetization vector.

I. INTRODUCTION

In a few short years, microrobots will become the gold standard in a variety of industrial, medical, and academic applications. Some of the more important of these applications include minimally invasive surgery [1], drug delivery [2], microscale transport [3], and microscale assembly [4, 5]. Microrobots are heavily influenced by viscous forces since their length scale renders inertia forces irrelevant [6]. To compensate for a lack of inertia, significant work has been done to create particles that are driven using a variety of different modalities, such as through rotational magnetic fields [7], magnetic gradients [8], chemical reactivity [3, 9], thermal gradients [10], optical stimulation [11], and bacterial hybridization [12]. In the category of chemically driven microrobots, Janus particles have gained significant value due to the diverse dynamical effects that can arise during their fabrication. Janus particles are fabricated to consist of two hemispheres: one side has magnetic coating, such as cobalt, while the other side is coated with platinum. When the particles are suspended inside a hydrogen peroxide solution, the platinum will act as a catalyst and decompose any surrounding hydrogen peroxide; this causes a Janus particle to self-propel within the solution [13]. By using a static magnetic

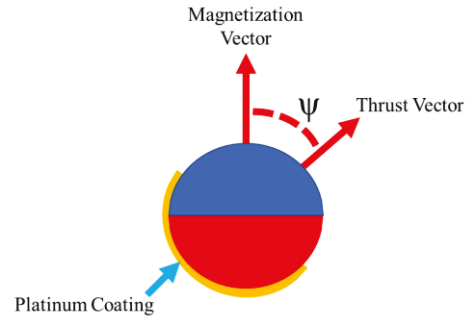


Figure 1. 2D Schematic of a Janus particle consisting of a cobalt magnetic core and a platinum coating. The thrust vector will always be on the side with a platinum coating. The magnetization vector, while in some cases occurs coincident to the thrust vector, will often have an offset angle ψ . This results from variations during fabrication. The blue and red parts of the sphere represent the north and south poles respectively.

field controller, the particles can be reoriented to create non-trivial trajectories. This has been discussed in several published works [13-16]. However, due to differences in magnetization, the magnetic orientation of a Janus particle may not coincide with the propulsion direction; this is shown graphically in Fig. 1. While open loop control of Janus particles with randomly oriented magnetization direction was discussed in [15], and closed loop control of coincidental magnetization has been discussed in [16]; there has been no effort yet to develop, or understand the effects of closed loop performance with randomly oriented particles. In this paper, we apply a closed loop controller to Janus particles that possess misaligned magnetic orientations to the propulsion vector and compare their responses when performing simple trajectories. We examine particles with magnetization offsets of only a few degrees all the way to a perfectly perpendicular offset of 90° . We also explore the effect that a misaligned magnetization axis plays in open loop 3D motion. In section II) we discuss the fabrication of the Janus particles, the closed loop control dynamics, and experimental setup. In section III) we give an overview of the results comparing randomly oriented Janus particles to coincidental particles. In section IV) we present our conclusions and future work.

II. FABRICATION AND EXPERIMENTAL OVERVIEW

A. Janus Particle Fabrication

This section overviews the fabrication of catalytic Janus particles. Fig. 2 (a) gives a brief visual summary of the Janus particle fabrication process, from initial etching of the

*Research supported by the NSF Foundation

Louis William Rogowski, Xiao Zhang, Anuruddha Bhattacharjee, Jung Soo Lee, and Min Jun Kim are with Southern Methodist University, Dallas, TX 75206 USA phone: 214-768-3972; fax: 214-768-1473; e-mail: mjkim@tyle.smu.edu.

Li Huang and Aaron Becker are with the University of Houston, Houston, TX 77204 USA.

polystyrene beads, to the multilayer coatings of both platinum (Pt) and cobalt (Co). To start, a 0.5%(w/w) polystyrene bead water solution was prepared using polystyrene beads (Spherotech, IL) that were 5 μm in diameter. The beads were coated as a monolayer on a glass slide whose surface was cleaned using UV-Ozone. The UV-Ozone treatment makes the glass surface hydrophilic, allowing the aqueous solution to spread out evenly along the slide's surface. As the water dried, the beads organized into a monolayer, with each bead touching side by side in a cluster through a self-assembled monolayer (SAM) effect. This can be seen in Fig. 2 (b). The beads were not individually distributed on the surface. Reactive ion etching (RIE) was applied to separate the clustered polystyrene beads from each other by etching the bead surface uniformly (Fig. 2(b)). O₂ plasma, with a relatively high pressure (250 mTorr) and low power (50 W), was used to gently etch the surface into a round shape [17]; it takes about 10 min to reduce a 5 μm polystyrene bead to 2.5 μm which is about the half of the original size. To fabricate Janus particles which possessed both characteristics of magnetism and catalytic propulsion, both Co and Pt were coated on each half of the beads using an e-beam thermal evaporator (Temescal CV-8 e-beam evaporator). Multilayer Janus particles were prepared to create stronger magnetism effects [18]; there were five coating layers total in the sequence of Pt 3nm, Co 3nm, Pt 3nm, Co 3nm, and Pt 3nm. The Pt and Co were evaporated at a slow rate of 0.02 nm/sec to ensure the high quality deposition. Only half of the surface was coated with platinum, by which the Janus particle catalyzed H₂O₂ decomposition and caused catalytic propulsion during experiments. The final Janus particles can be seen in Fig. 2(c). The attached beads could be easily detached from the glass surface through a gentle washing with water; we also gently stroked the coated surface with a paint brush to help release the particles. The scanning electron microscopy (SEM) image of the multilayer Janus particles was acquired in Fig. 2(d). The final size of the Janus particles is approximately 6 μm .

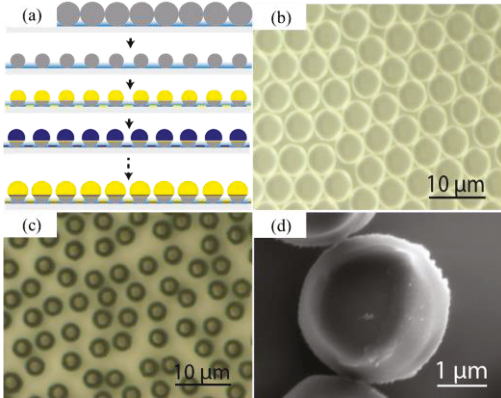


Figure 2. (a) Multilayer Janus particle fabrication steps using Co/Pt layers. (b) Clustered polystyrene beads in a monolayer. (c) Separate multilayer Janus particles after RIE and Co/Pt capping. (d) SEM image of multilayer Janus particle.

B. Experimental Setup

An approximate Helmholtz coil system was used to produce static magnetic fields to orient the Janus particles. The governing equations for the magnetic field for 2D control can be seen in Eq. (1) where θ is the orientation direction and B_s is the magnitude of the static magnetic field. For all tests

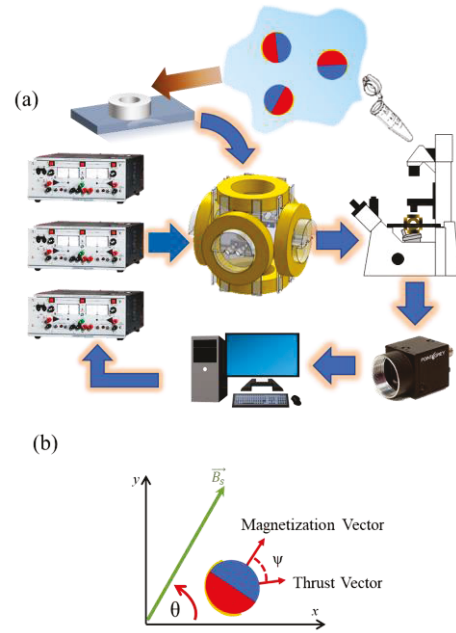


Figure 3. (a) Overview of experimental set up including Helmholtz coil system, sample chamber with Janus particles, microscope, power supplies, camera, and computer. (b) The graphical effect Eq. (1) has on the static magnetic field vector. The Janus particle will naturally orient its magnetization vector to the static magnetic field vector; this doesn't guarantee propagation direction however.

discussed in this paper, 5 Volts were applied to the coils which resulted in a static field of 8 mT; this field was only used to orient the particles and did not create any magnetic field gradients. Janus particles of 6 μm diameter were inserted into a Polydimethylsiloxane (PDMS) chamber approximately 2 mm in diameter and 1 mm thick, which was bonded to a glass slide. A 5 μm solution of concentrated Janus particles was placed into the chamber and then mixed with a diluted 10% H₂O₂ solution (Sigma Aldrich). A cover slide was then applied to enclose the sample chamber to minimize internal flow. This chamber was then placed in the center of the approximate Helmholtz coil system. Using three programmable power supplies (KEPCO, BOP 36-6M) interfaced with two digital acquisition control boards (BNC-2110), and a customized LabVIEW program, the particles could be manipulated based on the formulas presented in Eq. (1). All videos were captured and processed using a CMOS camera at 30 frames per second (fps). The experimental setup can be seen in Fig. 3 (a), while the effect θ has on the static magnetic field can be seen in (b). Due to the decomposition of H₂O₂, the chamber would fill with bubbles, and interfere with image capturing over time. All samples were used until bubbles made it impossible to clearly view Janus particles or no usable Janus Particles could be located.

$$\mathbf{B} = \begin{bmatrix} -B_s \cos(\theta) \\ B_s \sin(\theta) \\ 0 \end{bmatrix} \quad (1)$$

B. Kinematics Modeling

To model the kinematics of Janus particles, we must first consider a Janus particle in a 2D plane with an offset angle θ_0 , measured counter-clockwise, from its magnetic moment axis to its velocity vector. Given an external magnetic field with the orientation angle $\theta(t)$, the Janus particle aligns to its magnetic moment with the external field, and the simplified kinematics at time t is described by Eq. (2) where $x(t) \in \mathbb{R}^{2 \times 1}$ denotes the position, and $\mathbf{v}(t) \in \mathbb{R}^{2 \times 1}$, seen in Eq. (3), denotes the velocity, and v represents the magnitude.

$$\mathbf{x}(t + \Delta t) = \mathbf{x}(t) + \mathbf{v}(t)\Delta t \quad (2)$$

$$\mathbf{v}(t) = v \begin{bmatrix} \cos(\theta(t) + \theta_0) \\ \sin(\theta(t) + \theta_0) \end{bmatrix} \quad (3)$$

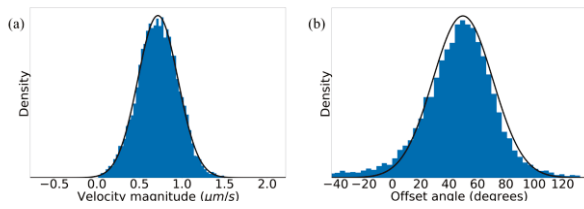


Figure 4. (a) Velocity magnitude distribution of sampled Janus particles. (b) Offset angle distribution of sampled Janus Particles.

Note the offset angle θ_0 is constant to each Janus particle, but this angle can be different between individual particles. To identify the velocity magnitude v and the offset angle θ_0 of a Janus particle, three experiments were performed with more than 10000 data points. Fig. 4 shows the histograms of velocity magnitude distribution and offset angle distributions. Based on their statistics, the average velocity magnitude is approximated as $0.717 \mu\text{m/s}$ with a standard deviation of 0.236 and the average offset angle was identified as 49.45° with a standard deviation of 21.132 . To validate the kinematics model, the simulation results were compared with experimental data, Fig. 5 demonstrates a particle with the same offset angle and similar velocity as the one predicted by the statistical model.

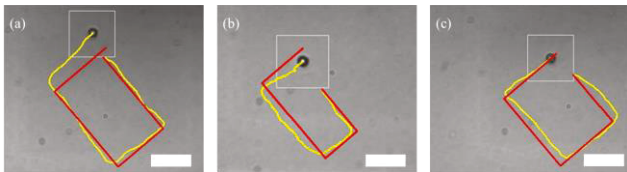


Figure 5. (a-c) The simulated trajectories of the particle are illustrated by the red line, while the actual path of the particle is shown in the yellow line. This particle closely matched the predictions given in the statistical analysis. By predetermining this offset angle, Janus particle motion can be predicted with a high degree of accuracy. Scale bars are $10 \mu\text{m}$.

C. Feedback Control Dynamics

The feedback control used in this paper is identical to the one utilized to maneuver achiral microrobots in previous research [19-21], however, in this case, it is significantly simplified to

only care about the change in θ . This simplification was performed since the Janus particles would move with a semi-constant velocity when exposed to H_2O_2 and did not rely on rotational dynamics to move through the fluid medium. The time derivative of θ can be seen mathematically in Eq. (4). Where, k is a gain parameter and α is the difference between the direction of the desired position relative to the Janus particle φ , and the magnetic heading angle θ of the Janus particle. The precise equation for α can be seen in (5). Throughout our experiments, k was set to a constant value of 5. More complex controllers will be developed in future work to create more precise control modalities.

$$\dot{\theta} = k\alpha \quad (4)$$

$$\alpha = \varphi - \theta \quad (5)$$

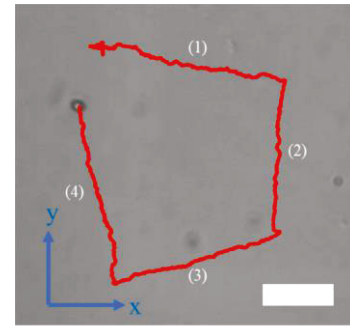


Figure 6. Trajectory of a heterogeneous particle with a small offset angle. The static magnetic fields applied are oriented to 0° , 90° , 180° , and 270° at points (1-4) respectively. The particle could reliably follow the static magnetic field direction. Scale bar is $10 \mu\text{m}$

III. RESULTS

The results section will be broken up into three sections: the first section will discuss a homogeneous Janus particle, where the magnetization vector was closely aligned to the propulsion vector; the second will discuss heterogeneous particles, where a larger offset value of was present; and the third will discuss open loop 3D control of a heterogeneous Janus particle.

A. Homogeneous Particles

Homogeneous particles performed exceptionally well when exposed to static magnetic fields and their motion was highly consistent with the magnetic field direction. In Fig. 6, we demonstrate a particle moving in a box pattern when

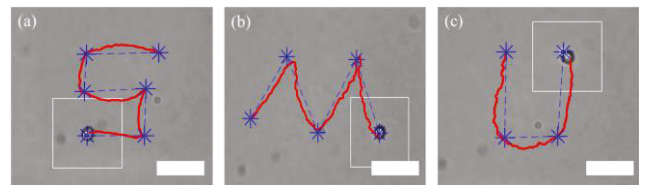


Figure 7. Arbitrary closed loop trajectories of a Janus particle with a small offset angle. This particle could easily navigate towards the intended targets without issue. The blue dots represent the target points, the dashed lines represent the desired trajectory, and the red solid line shows the actual trajectory. The white box is used to track the particle. The scale bars are $10 \mu\text{m}$.

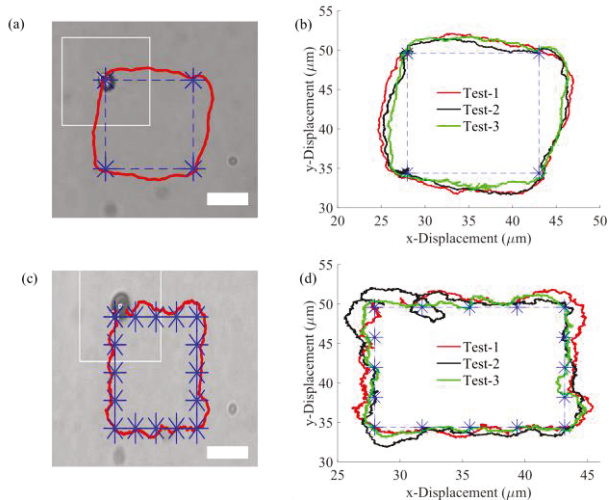


Figure 8. (a) Closed loop control of Janus particle to form a box shape pattern. Blue dashed line represents desired path and blue stars represent target points. The solid red line indicates the actual path followed by the particle. The particle started at the top left point and proceeded counter clockwise to each target point. (b) Shows three independent trajectories of the Janus particle under the same control inputs and similar starting conditions. All trials demonstrated nearly identical trajectories. (c) A box trajectory of the same size as (a) but with 20 points bounding the box. (d) Trajectories of the Janus particle navigating the box outlined in (c). Increasing the number of points greatly improved the particles trajectory accuracy. Deviancy between trials was caused by tracking failures or from focal plane shifting. Scale bars in (a) and (c) are 10 μm .

exposed to static magnetic fields applied at the angles 0° , 90° , 180° , and 270° using open loop control. While there is a slight offset angle present, the particle could still move in the intended direction with only small variation. When a similar particle was controlled using the discussed feedback controller, it displayed high accuracy, especially when asked to perform arbitrary trajectories. An example of these trajectories can be seen in Fig. 7. When examined for trajectory repeatability, the particle was directed to perform a box pattern with target points positioned $16 \mu\text{m}$ apart. An example of this trajectory can be seen in Fig. 8 (a). While the example does not perfectly follow the desired direction, it does indeed reach each of the target destinations without significant issue. Three independent tests were performed, and each test produced near identical trajectory results and can be seen in Fig. 8 (b); any variations were caused by slight differences in initial starting position and tracking failures using real time image processing. When these trajectories were increased from 4 points to 20 points, with a $4 \mu\text{m}$ gap between each point, the particle was able to more closely approximate the box pattern as can be seen in Fig 8 (c). However, as can be seen in Fig. 8 (d), the results were not without their issues. Test-3 in Fig. 8 (d) was particularly deviant, where the Janus particle often strayed far from the desired trajectory and in one case completely circling the target point. This can be attributed to error in the timing associated with incrementing the target positions after the Janus particle finished approaching the previous target. In the other two cases though, the particle was close enough in proximity to the desired path to be considered acceptable. Similar results were obtainable for other Janus particles with low offset angles.

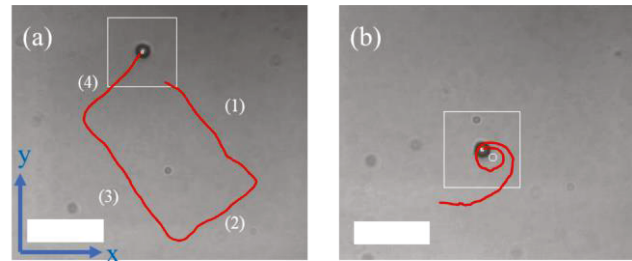


Figure 9. (a) Arbitrary closed loop trajectories of a Janus particle with a large offset angle of approximately 45° . The static magnetic fields applied are oriented to 0° , 90° , 180° , and 270° at points (1-4) respectively. (b) Closed loop control of the particle. Instead of directly approaching the target white circle, the particle spirals in a decaying orbit towards it. While not a perfect control of the particle, this effect can create more unique motion effects that could be useful in robotics applications. The white box is used to track the particle. The scale bars are 10 μm .

B. Heterogeneous Particles

A heterogeneous particle with an approximate offset angle of 45° was identified through open loop control. Using open loop control, a static magnetic field direction of 0° , 90° , 180° , and 270° was applied; the resulting trajectory can be seen in Fig. 9 (a). Since the box produced was tilted, a 45° offset angle was estimated to have caused the deviation. Applying the closed loop control algorithm to a single point resulted in a spiral towards the target point, this can be seen in Fig. 9 (b). While the offset angle prevents the Janus particle from directly reaching the target; given enough time, the particle's spiral will decay and allow for proximity to the target. While this is not optimal, it can still create interesting effects when directed to perform the same box trajectories carried out using

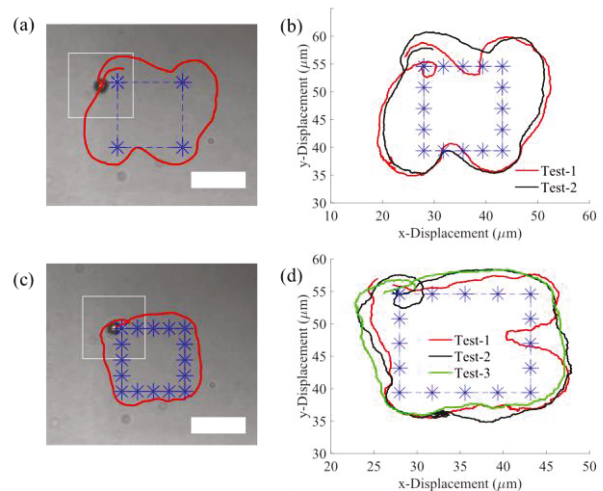


Figure 10. (a) Closed loop control of a Janus particle with a 45° offset forming a box shape pattern. Blue dashed line represents desired path and blue stars represent target points. The solid red line indicates the actual path followed by the particle. The particle started at the top left point and proceeded counter clockwise to each target point. (b) Shows two independent trajectories of the Janus Particle under the same control inputs and similar starting conditions. (c) A box trajectory of the same size as (a) but with 20 points bounding the box. (d) Trajectories of the Janus particle navigating the box outlined in (c). The particle had improved accuracy in following the intended trajectory, but the offset angle made directly reaching the targets, without spiraling, unlikely. Scale bar in (a) is 10 μm .

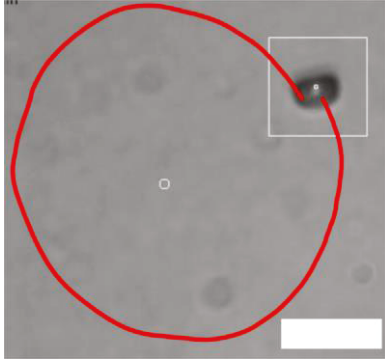


Figure 11. A Janus particle with a 90° magnetization offset to the thrust vector. This particle will never reach the target point indicated by the white circle, and instead will orbit almost perfectly around it. The scale bar is $10\ \mu\text{m}$ and the white box tracks the particle.

the homogeneous particle. These trajectories can be seen in Fig. 10 (a-b) for four target point locations and Fig. 10 (c-d) for 16 target points. The points had to be iterated fast enough to prevent the particle from spiraling around any given target point. Interestingly, while the four-point box in Fig. 8 (a) was inaccurate, the particle performed very similar trajectories between the independent trials in Fig. 8 (b). Going from a four point box to a 16 point box greatly improved the trajectory accuracy of the particle, with only one noticeable discrepancy during Test-1 in Fig. 8 (d), where the particle overshot the target and went inside the box.

In another experiment, a particle was identified with a large offset angle of approximately 90° in relation to the thrust vector. This can be seen in Fig. 11. Under closed loop control, the particle almost perfectly orbits around the white target point; never approaching the target or experiencing a decay in its orbit. The slight offset from the start position to the end was the result of a tracking failure. It is unclear yet if a Janus particle could possess an offset angle greater than 90° ; if such a particle does exist, it would spiral away from the target point with an increasing orbit.

C. 3D Motion of Heterogenous Janus Particles

Janus particles with an offset in the magnetization vector could undergo 3D motion when a static magnetic field in the Z direction was applied; this re-oriented the particle to have its propulsion vector pointed upward away from the substrate. To track the motion of the particle in the z-direction, the particles pixel area was tracked using image processing. As the focal plane was gradually shifted away from the particle, the pixel area of the particle would proportionally increase. Using a simple 1st order approximation, the area was correlated to z-height in the curve shown in Fig. 12 (c). A trajectory of the particle can be seen in Fig. 12(a), where the particle was directed to perform directions under static magnetic fields in the 0° , 90° , 180° , and 270° directions. When applying the z-height estimation curve seen in Fig. 12 (c), the 3D motion trajectory of the particle can be viewed in Fig. 12 (b). While there is some error associated with this estimation, due to random variations in particle area from image processing, the 3D trajectory can still be treated as a realistic interpretation of the particle's trajectory. The offset angle associated with the particle did not have any significant negative impact on its' 3D

motion; however, based on what we saw in previous sections, particles with larger offset values would experience a very slow ascent time, or none at all in the case of a 90° offset. Unfortunately, locating particles that could move in the z-direction with sufficient thrust was a challenge, as often times the particles themselves did not possess enough propulsive power to overcome the gravitational force. This will be addressed in future work by modulating the surrounding fluid properties to increase density.

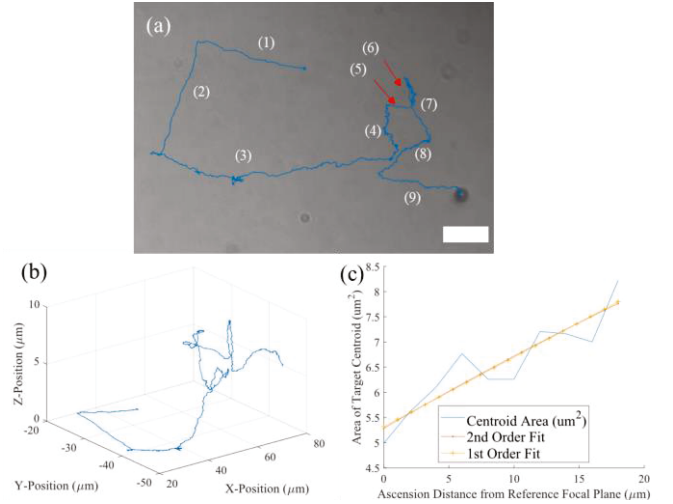


Figure 12. (a) Trajectory of a heterogeneous particle. The applied static magnetic field was 0° , 90° , 180° , 270° , 180° , 270° , 90° , 0° , and 180° at points (1-9) respectively. (b) The estimated 3D trajectory of the particle. (c) A linear and second order fit to the change in pixel area as the particle moved further away from the initial focal plane. Scale bar is $10\ \mu\text{m}$.

IV. CONCLUSION

In conclusion, we demonstrate that heterogeneous particles can be manipulated using feedback control and can perform simple 3D trajectories. For the feedback control, the magnetization angle played a huge impact on how well the Janus particles could reach their target destinations. If the magnetization angle was close to the propulsion vector, the particle could reach the intended target with little hinderance. However, if the offset angle was significant, the particle would take significantly longer to reach the target and proceed towards it in a spiral motion. When the offset angle was 90° , the particle will almost perfectly orbit the intended target position. When the particles were directed to perform a box pattern, heterogeneous particles could perform the intended trajectories, with improving accuracy as the number of points bounding the box trajectory increased. Of course, in both Janus particles with large and small offset angles, there were abnormal cases where issues in tracking or variations in starting conditions caused the particles to behave unexpectedly. Heterogeneous particles were also demonstrated to show 3D motion and could perform arbitrary trajectories. Overall, heterogeneous Janus particles were able to not only perform reasonably well under feedback control but also could perform reasonable 3D motions without

significant issue. In future work, we plan to implement a feedback controller which can retroactively account for the magnetization angle difference and perform 3D feedback control of a heterogeneous Janus particle.

ACKNOWLEDGMENT

This work was funded by the National Science Foundation (CMMI 1619278 and 1737682). We would like to thank Dr. U Kei Cheang and Dr. Jamel Ali for their guidance during the experimental setup and for laying the groundwork to make this research possible.

REFERENCES

- [1] B. J. Nelson, I. K. Kaliakatsos, and J. J. Abbott, "Microrobots for minimally invasive medicine," *Annual review of biomedical engineering*, vol. 12, pp. 55-85, 2010.
- [2] S. Lee, S. Kim, S. Kim, J. Y. Kim, C. Moon, B. J. Nelson, *et al.*, "A Capsule - Type Microrobot with Pick - and - Drop Motion for Targeted Drug and Cell Delivery," *Advanced healthcare materials*, vol. 7, p. 1700985, 2018.
- [3] S. Sanchez, A. A. Solovev, S. Schulze, and O. G. Schmidt, "Controlled manipulation of multiple cells using catalytic microrobots," *Chemical Communications*, vol. 47, pp. 698-700, 2011.
- [4] S. Martel and M. Mohammadi, "Using a swarm of self-propelled natural microrobots in the form of flagellated bacteria to perform complex micro-assembly tasks," in *Robotics and Automation (ICRA), 2010 IEEE International Conference on*, 2010, pp. 500-505.
- [5] G. Zhang and D. Wang, "Colloidal lithography—the art of nanochemical patterning," *Chemistry—An Asian Journal*, vol. 4, pp. 236-245, 2009.
- [6] E. M. Purcell, "Life at low Reynolds number," *American journal of physics*, vol. 45, pp. 3-11, 1977.
- [7] T. Honda, K. Arai, and K. Ishiyama, "Micro swimming mechanisms propelled by external magnetic fields," *IEEE Transactions on Magnetics*, vol. 32, pp. 5085-5087, 1996.
- [8] B. G. Hosu, K. Jakab, P. Bánki, F. I. Tóth, and G. Forgacs, "Magnetic tweezers for intracellular applications," *Review of Scientific Instruments*, vol. 74, pp. 4158-4163, 2003.
- [9] J. Simmchen, V. Magdanz, S. Sanchez, S. Chokmaviroj, D. Ruiz-Molina, A. Baeza, *et al.*, "Effect of surfactants on the performance of tubular and spherical micromotors—a comparative study," *RSC advances*, vol. 4, pp. 20334-20340, 2014.
- [10] B. Qian, D. Montiel, A. Bregulla, F. Cichos, and H. Yang, "Harnessing thermal fluctuations for purposeful activities: the manipulation of single micro-swimmers by adaptive photon nudging," *Chemical Science*, vol. 4, pp. 1420-1429, 2013.
- [11] K. C. Neuman and A. Nagy, "Single-molecule force spectroscopy: optical tweezers, magnetic tweezers and atomic force microscopy," *Nature methods*, vol. 5, p. 491, 2008.
- [12] J. Ali, U. K. Cheang, J. D. Martindale, M. Jabbarzadeh, H. C. Fu, and M. J. Kim, "Bacteria-inspired nanorobots with flagellar polymorphic transformations and bundling," *Scientific reports*, vol. 7, p. 14098, 2017.
- [13] S. Das, E. B. Steager, K. J. Stebe, and V. Kumar, "Simultaneous control of spherical microrobots using catalytic and magnetic actuation," in *Manipulation, Automation and Robotics at Small Scales (MARSS), 2017 International Conference on*, 2017, pp. 1-6.
- [14] S. Das, A. Garg, A. I. Campbell, J. Howse, A. Sen, D. Velegol, *et al.*, "Boundaries can steer active Janus spheres," *Nature communications*, vol. 6, p. 8999, 2015.
- [15] S. Das, E. Steager, M. Ani Hsieh, K. J. Stebe, and V. Kumar, *Experiments and open-loop control of multiple catalytic microrobots* vol. 14, 2018.
- [16] I. S. Khalil, V. Magdanz, S. Sanchez, O. G. Schmidt, and S. Misra, "Precise localization and control of catalytic Janus micromotors using weak magnetic fields," *International journal of advanced robotic systems*, vol. 12, p. 2, 2015.
- [17] B. Malekian, K. Xiong, G. Emilsson, J. Andersson, C. Fager, E. Olsson, *et al.*, "Fabrication and Characterization of Plasmonic Nanopores with Cavities in the Solid Support," *Sensors*, vol. 17, p. 1444, 2017.
- [18] L. Baraban, D. Makarov, R. Streubel, I. Monch, D. Grimm, S. Sanchez, *et al.*, "Catalytic Janus motors on microfluidic chip: deterministic motion for targeted cargo delivery," *ACS nano*, vol. 6, pp. 3383-3389, 2012.
- [19] U. K. Cheang, M. Dejan, J. Choi, and M. Kim, "Towards model-based control of achiral microswimmers," in *ASME 2014 Dynamic Systems and Control Conference*, 2014, pp. V002T33A002-V002T33A002.
- [20] U. K. Cheang, H. Kim, D. Milutinović, J. Choi, and M. J. Kim, "Feedback control of an achiral robotic microswimmer," *Journal of Bionic Engineering*, vol. 14, pp. 245-259, 2017.
- [21] U. K. Cheang, H. Kim, D. Milutinović, J. Choi, L. Rogowski, and M. J. Kim, "Feedback control of three-bead achiral robotic microswimmers," in *Ubiquitous Robots and Ambient Intelligence (URAI), 2015 12th International Conference on*, 2015, pp. 518-523.